Open Access

Recent Progress in Materials

LIDSEN Publishing Inc.

Original Research

Application of the Extrapolation Method in Battery Diagnostics for Electric Vehicles

Oleksandr Beshta [1], Gennadiy Pivnyak [1], Oleksandr Beshta Jr [1], Roman Borovik [1], Cáceres Cabana Edgar [2], Adam Smolinski [3,*]

1. Dnipro University of Technology, Dnipro, Ukraine; E-Mails: beshtaa@nmu.one; pgg@nmu.one; beshta.o.o@nmu.one; borovyk.r.o@nmu.one
2. Universidad Nacional de San Agustin de Arequipa, Peru; E-Mail: ecaceresca@unsa.edu.pe
3. Central Mining Institute, Katowice, Poland; E-Mail: smolin@gig.katowice.pl

* **Correspondence:** Adam Smolinski; E-Mail: smolin@gig.katowice.pl

Academic Editor: Sawanta S. Mali

Special Issue: Advanced Nuclear Magnetic Resonance in Batteries and Fuel Cells Research

Recent Progress in Materials
2022, volume 4, issue 4
doi:10.21926/rpm.2204023

Received: August 17, 2022
Accepted: October 20, 2022
Published: November 14, 2022

Abstract

In a lithium-ion battery, the crossing of its charging–discharging curves represents an unambiguous current capacity. The reproduction of a complete charging–discharging cycle defines the maximum possible charge for a current battery state. When obtaining of the curves experimentally, one should consider the duration of polarization or depolarization. It is reported that the battery capacity depends considerably on the value of the battery's internal resistance as this value defines the location of the actual charging–discharging curves relative to the nominal curves, i.e., the point of their crossing shifts. The present study aimed to develop a diagnostic algorithm for the batteries of electric vehicles for a complete charge–discharge cycle, considering the processes of polarization and depolarization. The mathematical expressions for determining the internal resistance and the complete charge of the battery were obtained. The novelty of the present study is in the fact that by applying extrapolation to a simple electrical model of a lithium-ion battery, the degree of degradation

and the current charge could be predicted without the requirement of lengthy experimental procedures.

Keywords
Lithium-ion battery; capacity; degradation; charging-discharging

1. Introduction

Lithium-ion batteries are among the main driving forces of advancements in the field of technology. The two major application areas of lithium-ion batteries are electric vehicles and energy storage systems. Since the application of lithium-ion batteries as power sources is only increasing with time, improving the technology for diagnosing lithium-ion batteries becomes important.

The application of lithium-ion batteries demands the fulfillment of certain conditions of the charging–discharging cycle. In a lithium-ion battery, in addition to the reversible processes of the formation of lithium-ion flux, certain irreversible electrochemical and chemical reactions occur as well. As a consequence, the discharge capacity in each cycle is less than the discharge capacity in the previous stage of charging, which represents the degradation of a lithium-ion battery [1]. Accordingly, an increasing number of cycles (a cycling process) results in the degradation of electrodes and an increased degradation rate [2]. The degree of degradation may, therefore, be assessed according to the charging–discharging characteristics, as battery voltage depends on the number of cycles or amperes spent per hour during a charging/discharging process [3].

The nature of the different irreversible processes results in differences in the degradation levels [4]. Previous studies have reported various reasons for electrode degradation: the loss of the active substance (solution, cracking, and layering) [5], an increase in the internal resistance of the battery (formation of passive films) [6], different structural changes in the active material, which alter the energy range of the lithium insertion [7], etc. Accordingly, the following are stated as the possible mechanisms underlying the degradation process [2]:

- the loss of the active substance in the electrodes does not change the form of the charging–discharging curves;
- increasing the internal resistance of a battery (electrodes) causes a shift in the charging–discharging curve in parallel to its coordinate axis [8];
- changes in the structure of the electrodes result in considerable changes in both form and characteristics of the charging–discharging curves.

2. Materials and Methods

In order to assess the technical state of batteries, their ability to accumulate and release energy, their lifetime, and certain other parameters, are assessed. One of these parameters is SOC (state of charge), which represents the battery charge. However, studies have used different methods for the determination of this parameter. For instance, one study [9] defined SOC as the ratio of the maximum possible battery charge to the nominal battery charge value and used the method recommended by the manufacturer to determine the SOC value. In this context, the present study addressed the complexity of obtaining an accurate SOC value due to a series of factors that cause

significant variability in the values of both the maximum possible battery charge and nominal battery charge. Moreover, this complexity renders it almost impossible to use SOC to control the existing value of the battery charge. In a study [4], SOC was defined as the parameter for characterizing the degree or the state of charge of a battery and was calculated using the equation provided below.

$$SOC(t) = \frac{Q(t)}{Q_{max}} 100\%, \tag{1}$$

In the above equation, $Q(t)$ is the existing battery charge and Q_{max} is the maximum possible battery charge considering the technical state of the battery.

If t is the present charging time, then:

$$Q(t_c) = Q_0 + \int_0^{t_c} I(t)dt\,, \tag{2}$$

where, Q_0 denotes the battery charge at the beginning of the charging process, $I(t)$ denotes the charging current, and t_c denotes the charging time.

In the case of discharge,

$$Q(t) = Q_0 - \int_0^{t_{dc}} I(t)dt\,, \tag{3}$$

where, Q_0 denotes the battery charge at the beginning of the discharging process, $I(t)$ denotes the discharging current, and t_{dc} denotes the discharging time.

The determination of the SOC value using the formulas (1) to (3) is beneficial from the perspective of the evaluation of the existing battery charge as well as the degree of degradation of the battery.

DOD (Deep of discharge) is the complete analog of SOC and reflects the discharge depth. The value of this parameter is, therefore, calculated as below:

$$DOD(t) = \ 100\% - SOC(t), \tag{4}$$

The parameter SOH (State of Health) reflects battery health. However, no single-valued index is currently used for reflecting the state of battery health. Since the main criterion for battery performance is the capacity of the battery to provide maximum charge $Q_{max}(t)$, the comparison of this criterion with the certified value Q_N, which is determined by the battery manufacturer, is used for calculating SOH, as follows:

$$SOH(t) = \frac{Q_{max}(t)}{Q_N} 100\%. \tag{5}$$

Consequently, to evaluate the change in the technical state of a battery, it becomes necessary to calculate the value of the existing battery charge and the maximum possible value of this parameter.

Since the charge value is an integral characteristic of the charging (discharging) rate, the value of battery charging (discharging) may be calculated in amperes per hour (Ah).

3. Results and Discussion

Special equipment based on radioactive permeability is used for assessing the condition of lithium-ion batteries [10]. In order to estimate the charging value of a battery, it is necessary to develop a certain model of the electrochemical charging (discharging) process. Dynamic models of the *Thevenin equivalent circuit* type [4] are the most used ones in this context. This kind of model describes the processes occurring in a lithium-ion battery based on the elements in the electrotechnical circuit (Figure 1) [9]. In these models, the electric resistance R_0 determines the internal resistance of the battery and is responsible for the two main processes occurring within the battery, namely, intercalation and deintercalation.

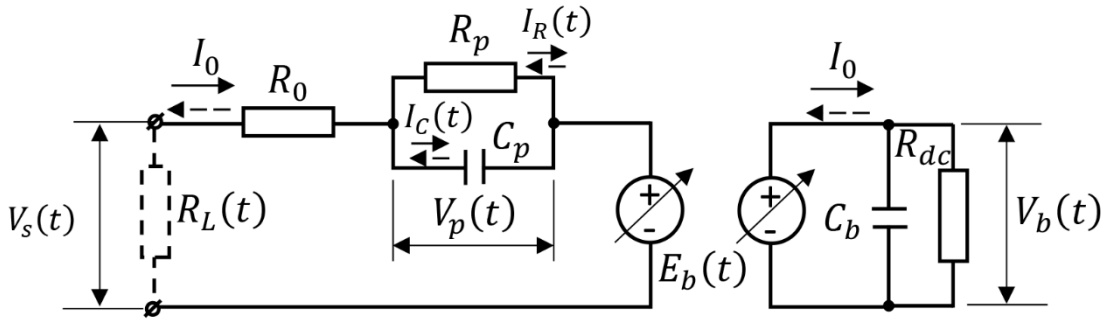

I_0-constant current, *t*-time, *R0*-internal resistance, *Rdc*-active resistance, *Cb*-battery capacity, *Cp* and *Rp*- resistance and capacity of the polarization process, *Ic*-capacity current, *Vp*-voltage of the polarization process, *Vb*-battery voltage, *Eb*-battery EMF

Figure 1 Equivalent circuit for the dynamic model of a battery.

One of the mechanisms reported for lithium intercalation into graphite is the sequential filling of the gap between the graphene layers with lithium. This process provides battery charging. The process of deintercalation is opposite to the intercalation process and occurs during battery discharging. Accordingly, one intercalation–deintercalation represents one cycle of battery operation. The internal resistance R_0 characterizes the degree of degradation of the battery during this cyclic process [11]. If battery degradation occurs due to certain reasons, it reflects in an increase in the internal resistance R_0.

The resistance R_p and capacity C_p characterize the transient process of polarization – a process of the development of a flux of positive lithium ions electrode-to-electrode. This polarization process occurs each time a battery switches on for charging or discharging.

In the *Thevenin equivalent circuit* model, the mechanisms underlying the intercalation and deintercalation processes are determined by the processes of charging and discharging of capacity C_b, while the mechanism of natural charge leakage is determined by the voltage of the losses in active resistance R_{dc}.

According to the circuit depicted in Figure 1, it is possible to achieve a balance of voltages while the battery is charging and discharging at a constant current ($I_0 = const$) [12].

3.1 Charging

When a battery is charged with a constant current, i.e., $I_0 = const$, after a certain time t, the battery has charge $Q = I_0 \cdot t$. Accordingly, the balance of voltages relative to the parameter Q would be as follows:

$$V_b^{ch}(Q) = I_0 R_0 + V_p(Q) + E_b^{ch}(Q), \tag{6}$$

where, $V_b^{ch}(Q)$ denotes the voltage when the capacity reaches the value C_b while charging, $E_b^{ch}(Q)$ is the EMF of the battery while charging, and $V_p(Q)$ denotes the voltage at capacity C_p.

A battery begins its charging process with the commencement of the polarization process.

3.1.1 Polarization Process

The circuit branches with elements C_p and R_p are defined as follows:

$$I_0 = I_R(t) + I_C(t), \tag{7}$$

where,

$$I_R(t) = \frac{V_p(t)}{R_p}; \tag{8}$$

$$I_C(t) = C_p \frac{dV_p(t)}{dt}. \tag{9}$$

Therefore, by using the formulas (7) to (9), a differential equation of the following form is obtained for the process of polarization:

$$I_0 R_p = T_p \frac{dV_p(t)}{dt} + V_p(t), \tag{10}$$

where, $T_p = C_p R_p$ is the time constant for the polarization process.

A complete solution of the above equation provides the following equation:

$$V_p(t) = I_0 R_p \left(1 - e^{-t/T_p}\right). \tag{11}$$

When the polarization process is over, the process of intercalation begins.

3.1.2 Intercalation Process

The intercalation process is defined by the following equation based on the capacity charging C_b:

$$I_0 = C_b \frac{dE_b^{ch}(t)}{dt}, \tag{12}$$

where, $E_b^{ch}(t)$ denotes the present EMF of the battery while charging.

Since charging is performed by means of the constant current I_0, it is possible to obtain the constant derivative EMF of the battery, which depends linearly on the charging time. The integration of equation (12) within the limits of charge Q_p *to* Q generates the following equation:

$$I_0 t = Q = C_b\left[E_b^{ch}(Q) - E_b^{ch}(Q_p)\right], \tag{13}$$

where, Q_p represents battery charging after the polarization process is over.

3.2 Discharging

A balance of voltages relative to the parameter Q while discharging is represented by the following equation:

$$V_b^{dc}(Q) = E_b^{dc}(Q) - I_0 R_0 - V_p(Q), \tag{14}$$

where, $V_b^{dc}(Q)$ denotes the voltage at capacity C_b while discharging, $E_b^{dc}(Q)$ is the EMF of the battery while discharging, and $V_p(Q)$ denotes the voltage at capacity C_p.

Discharging also begins with the process of polarization, as described by equation (11).

3.2.1 Deintercalation Process

The deintercalation process has a complete analog associated with capacity C_b, i.e., discharging. Therefore, using formula (12) within the range of discharge Q_p *to* Q, the following equation is obtained:

$$Q = C_b\left[E_b^{dc}(Q_p) - E_b^{dc}(Q)\right], \tag{15}$$

where, $E_b^{dc}(Q)$ is the present EMF of the battery while discharging.

In the charging and discharging cycle, the processes of intercalation and deintercalation occur under the conditions of the completed process of polarization or depolarization. Therefore, one could consider that, at $t \gg T_p$ ($Q \gg Q_p$), the following equation holds true:

$$V_p(Q) \approx I_0 R_p. \tag{16}$$

Accordingly, when $Q \gg Q_p$, the balance of the voltage for the process of charging (6) and that for the process of discharging (14) are defined as follows:

$$V_b^{ch}(Q) = I_0\left(R_0 + R_p\right) + E_b^{ch}(Q), \tag{17}$$

$$V_b^{dc}(Q) = E_b^{dc}(Q) - I_0\left(R_0 + R_p\right). \tag{18}$$

According to formulas (17) and (18), the voltage measured on the battery terminals differs from the EMF of the battery by the value of the voltage drop due to the internal resistance of the battery, $R_b = R_0 + R_p$. Accordingly, when the charging–discharging curves are defined by $V_b = f(Q)$ and the internal resistance is R_b, the equation $E_b = f(Q)$ unambiguously defines the level of charging–discharging and the degree of battery degradation.

The internal resistance of a battery may be determined using equation (17) or (18), depending on the curves used for depicting the charging or discharging process.

$$R_b = \left[V_b^{ch}(0) - E_b^{ch}(0)\right]/I_0\,, \tag{19}$$

$$R_b = \left[E_b^{dc}(0) - V_b^{dc}(0)\right]/I_0\,, \tag{20}$$

In the above equations, $E_b^{ch}(0)$ and $E_b^{dc}(0)$ are the EMFs of the battery prior to it being switched on for charging and discharging, respectively, while $V_b^{ch}(0)$ and $V_b^{dc}(0)$ denote the voltages on the battery terminals immediately after the battery is switched on for charging and discharging, respectively.

The theoretical curves for the charging $V_b^{ch}(Q)$ and discharging $V_b^{dc}(Q)$ of the battery depicted in Figure 2 correspond to the case when the amount of energy consumed for battery charging is equal to the amount of energy spent for battery discharging.

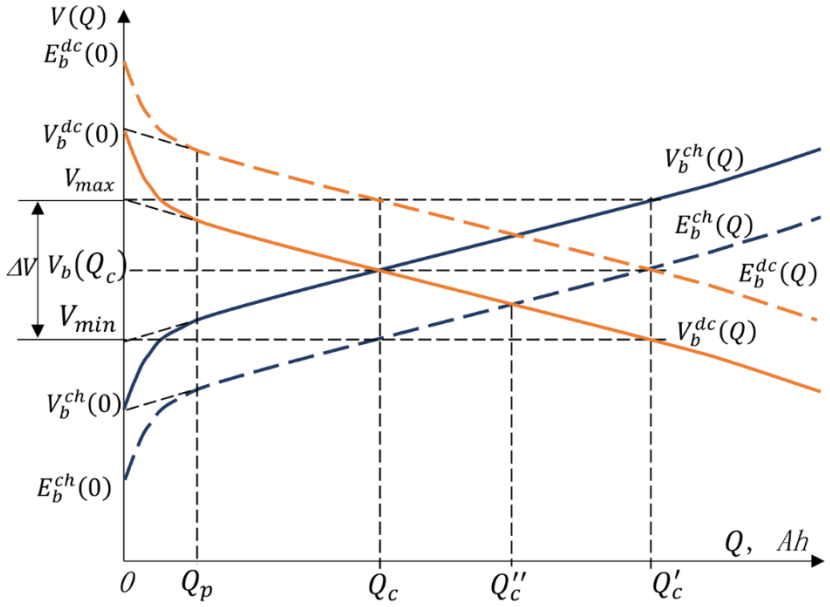

Qc-point of charging-discharging curves, V_b^{ch}, V_b^{dc}-battery voltage (charging, discharging), E_b^{ch}, E_b^{dc} – battery EMF (charging, discharging)

Figure 2 Curves for battery charging and discharging.

As visible in Figure 2, the curve for battery EMF while charging is located lower and in parallel to the curve of voltage, while the curve for battery EMF during discharging is in parallel and higher by the level of voltage I_0R_b. Since the extrapolated levels of voltages of the curves of charging V_{min} and discharging V_{max} are defined by means of equations (17) and (18) for $Q = 0$, the following equations hold true:

$$V_{max} = V_b^{dc}(0) - I_0R_b, \tag{21}$$

$$V_{min} = V_b^{ch}(0) + I_0R_b, \tag{22}$$

Accordingly, the following equation is obtained:

$$\Delta V = \left[V_b^{dc}(0) - V_b^{ch}(0)\right] - 2I_0R_b. \tag{23}$$

The difference ΔV is defined as the amount of present charge that the accumulator battery is capable of storing and releasing without any losses.

Using the formulas (21), (22), (17), and (18), one obtains the extrapolated curves for charging and discharging, which are as follows:

$$Q = C_b\left[V_b^{ch}(Q) - V_{min}\right], \tag{24}$$

$$Q = C_b\left[V_{max} - V_b^{dc}(Q)\right]. \tag{25}$$

Since point Q_c is determined as the point of crossing of the charging–discharging curves, then using the formulas (24) and (25) at $V_b^{ch}(Q_c) = V_b^{dc}(Q_c)$ generates the following equation:

$$2Q_c = C_b\left[V_b^{ch}(Q_c) - V_{min}\right] + C_b\left[V_{max} - V_b^{dc}(Q_c)\right] == C_b[V_{max} - V_{min}] + C_b\left[V_b^{ch}(Q_c) - V_b^{dc}(Q_c)\right] = C_b\Delta V. \tag{26}$$

Accordingly, the value of capacity without considering losses is calculated as follows:

$$C_b = \frac{2Q_c}{\Delta V}, [Ah/V]. \tag{27}$$

If ΔV reaches its maximum value, i.e., the battery is charged completely with the following discharge, then charge Q_c accounts for half of the complete battery charge without considering losses.

However, the battery charge may continue to compensate for losses in the battery during the discharge, at the internal resistance R_b, to the charge level Q_b' (Figure 2).

The crossing of the charging–discharging curves for the EMF, which corresponds to charge Q_b', is then obtained from equations (13) and (15). The extrapolation of the curves $E_b^{ch}(Q)$ and $E_b^{dc}(Q)$ onto the ordinate $V(Q)$ then generates the following equations:

$$E_b^{ch}\left(Q_p\right) = V_b^{ch}(0), \tag{28}$$

$$E_b^{dc}\left(Q_p\right) = V_b^{dc}(0). \tag{29}$$

Therefore, the following equations are obtained from formulas (13) and (15):

$$Q_c' = C_b'\left[E_b^{ch}(Q_c') - V_b^{ch}(0)\right], \tag{30}$$

$$Q_c' = C_b'\left[V_b^{dc}(0) - E_b^{dc}(Q_c')\right]. \tag{31}$$

Similar to the previous calculation, from formulas (30) and (31), considering $E_b^{ch}(Q_c') = E_b^{dc}(Q_c')$, the following equations are obtained:

$$2Q_c' = C_b'\left[E_b^{ch}(Q_c') - V_b^{ch}(0)\right] + C_b'\left[V_b^{dc}(0) - E_b^{dc}(Q_c')\right] = = C_b'\left[V_b^{dc}(0) - V_b^{ch}(0)\right] + C_b'\left[E_b^{ch}(Q_c') - E_b^{dc}(Q_c')\right] = C_b'[\Delta V + 2I_0R_b]. \tag{32}$$

i.e.,

$$C_b' = \frac{2Q_c'}{\Delta V + 2I_0R_b}, [Ah/V]. \tag{33}$$

Therefore, a battery with the capacity C_b' should be charged up to the level of charge Q_c', which corresponds to the voltage $V_b^{ch}(Q_c')$, to release the charge Q_c during discharging.

Since triangles $[V_{max}, V_b(Q_c), V_{max}]$ and $[V_b^{dc}(0), V_b(Q_c), V_b^{ch}(0)]$ are identical. It could be stated that:

$$C_b = C_b' = \frac{2Q_c}{\Delta V} = \frac{2Q_c'}{\Delta V + 2I_0R_b}, [Ah/V]. \tag{34}$$

However, the capacity indices C_b and C_b' are not valid for a real-life battery that has an internal resistance R_b and the associated losses. As depicted in Figure 2, after the battery discharge by a value of Q_c, a portion of charge $Q_c'' - Q_c$ remains in the battery. This charge arises as a compensation for the losses that occurred due to internal resistance, while charging.

This is why capacity C_b'' should be the capacity of a real-life battery, which is determined using the following formulas:

$$Q_c'' = C_b''\left[E_b^{ch}(Q_c'') - V_b^{ch}(0)\right], \tag{35}$$

$$Q_c'' = C_b''\left[V_{max} - V_b^{dc}(Q_c'')\right]. \tag{36}$$

Since for $E_b^{ch}(Q_c'') = V_b^{dc}(Q_c'')$, the following equation holds:

$$2Q_c'' = C_b''\left[E_b^{ch}(Q_c'') - V_b^{dc}(Q_c'')\right] + \left[V_{max} - V_b^{ch}(0)\right] = C_b''\left[V_{max} - V_b^{ch}(0)\right],$$

Accordingly, using the formulas (19) and (20), one obtains:

$$C_b'' = \frac{2Q_c''}{[V_b^{dc}(0) - V_b^{ch}(0)] - I_0R_b} = \frac{2Q_c''}{\Delta V + I_0R_b}, \tag{37}$$

where, $Q_c'' = \frac{Q_c' + Q_c}{2}$.

Next, using the formulas (27), (33), and (34), the following equation is obtained:

$$Q_c'' = Q_c\left(1 + \frac{I_0R_b}{\Delta V}\right). \tag{38}$$

Therefore, it could be concluded that $2Q_c'' = Q_b$ is the complete battery charge during maximum charging–discharging.

Formula (38) represents the interconnection between the complete battery charge Q_b, the internal resistance of the battery R_b, the difference between the resistance of the completely charged battery at the beginning of charging $V_b^{dc}(0)$, and the voltage of a completely discharged battery $V_b^{ch}(0)$.

If the reference (certified) data on the nominal battery charge of the given type $Q_{b,n}$ are available, then the comparison of the value Q_b, obtained using formula (38), enables the evaluation of the level of the real capacity and degradation degree of the battery being diagnosed.

Accordingly, the algorithm of battery diagnostics for a complete charging–discharging cycle is as follows:

1. At the initial moment, when the battery begins charging by means of direct current I_0 from the EMF level $E_b^{ch}(0)$, the voltage $V_b^{ch}(0)$ is measured.
2. After a certain duration, when the transient process of polarization is over, the battery is charged by the value of charge Q_p. This duration should be determined in advance using the reference battery.
3. The battery continues its charging up to the level that is admissible for that particular type of battery.
4. The transient process of depolarization is completed within a certain duration, which is equal to the duration of the polarization process. At this time point, the EMF level $E_b^{dc}(0)$ is measured.
5. At the initial moment of battery discharging by means of constant current ($\mathrm{I_0} = \mathrm{const}$), the voltage $\mathrm{V_b^{dc}}(0)$ is measured. The internal resistance $\mathrm{R_b}$ is calculated using the formula (20) and $\Delta \mathrm{V}$ is calculated according to the formula (23).
6. The battery continues its discharging for a time t_c up to the level of voltage $V_b^{dc}(Q_c) = V_b^{ch}(Q_c)$, and then, the voltage $Q_c = I_0 t_c$ is determined.
7. Charge Q_c'' is calculated according to formula (38).
8. Charge $2Q_c''$ is compared with the certified value $Q_{b,n}$. The real battery capacity is then determined.

Consider the experimental curves for the complete charging–discharging of two lithium-ion batteries for the electric vehicle *Leaf* with a specified rate $Q_{b,n} = 60\ \mathrm{Ah}$ at current $I_0 = 10\ \mathrm{A}$ (Figure 3).

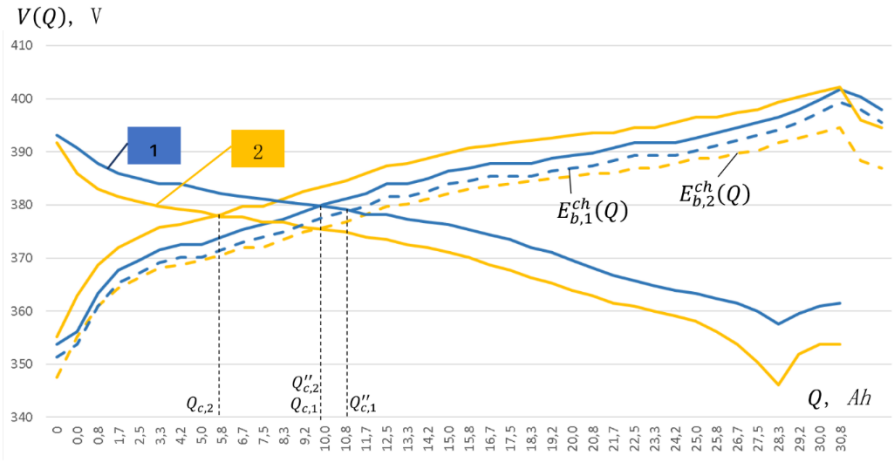

Qc-point of charging-discharging curves, $E_{b,1}^{ch}, E_{b,2}^{ch}$ – battery EMF (charging) 1st and 2d battery

Figure 3 Experimental curves for the charging–discharging of a battery for the electric vehicle 'Leaf'.

The data obtained using the algorithm presented above are provided in Table 1.

Table 1 Results of the experiments conducted with the batteries of '*Leaf*'.

# bat	$E_b^{dc}(0)$, V	$V_b^{dc}(0)$, V	$V_b^{ch}(0)$, V	R_b, Ohm	ΔV, V	Q_c, Ah	Q_c'', Ah	$C_b/C_{b,n}$.
1	393.12	390.72	356.16	0.24	29.76	10.0	10.8	0.36
2	392.73	385.92	362.88	0.681	9.42	5.8	9.993	0.33

According to Table 1, the capacities of battery 1 and battery 2 were 36% and 33%, respectively, of the certified battery. The graphics for the charging–discharging curves confirmed the correctness of the performed calculation (Figure 3). In the figure, the dotted lines indicate EMF $\mathrm{E}_{\mathrm{b},1}^{\mathrm{ch}}(\mathrm{Q})$ and $\mathrm{E}_{\mathrm{b},2}^{\mathrm{ch}}(\mathrm{Q})$ of the first and second battery, respectively.

4. Conclusions

The charging-discharging cycle of a battery may be assessed without conducting lengthy experimental procedures, using algorithms. In this context, the present study proposed a method, in which the current value of the charge and the battery capacity are obtained by determining the intersection of the charge–discharge curves without the requirement of conducting the entire cycle. Extrapolation of the curves for a complete charge–discharge cycle using this proposed method allows for obtaining the current value of the capacity and the degree of battery degradation in accordance with the passport values. It was revealed that, for data extrapolation, it is necessary to consider the duration of polarization of the charge and discharge process. For instance, in the case of the Leaf battery, this duration was 15–20 min. It is established that battery capacity is significantly affected by the internal resistance of the battery, which may be determined by comparing the curves obtained using the proposed method with the nominal curves, as the real charge–discharge curves are shifted relative to the nominal ones.

Author Contributions

Conceptualization, O.B., G.P., P.B.Jr, R.B., C.C. and A.S.; methodology, O.B., G.P., P.B.Jr; validation, O.B., G.P., P.B.Jr , R.B., C.C. and A.S.; formal analysis, O.B., G.P., P.B.Jr investigation, O.B., G.P., P.B.Jr, R.B.; writing—original draft preparation, O.B., G.P., P.B.Jr; writing—review and editing, O.B., G.P., P.B.Jr; visualization, O.B., G.P., P.B.Jr; supervision, A.S.

Competing Interests

The authors have declared that no competing interests exist.

References

1. Beshta O, Yermolayev M, Kaiser K, Beshta P, Taylor A. Limitations of the indirect field oriented control utilization for electric drives of pipeline valves. In: Energy efficiency improvement of geotechnical systems. London: CRC Press; 2013. pp. 29-38.
2. Lee S. Electrode-specific degradation diagnostics for lithium-ion batteries with practical considerations. Ann Arbor: University of Michigan; 2021.

3. Beshta OS, Kuvaiev MV. Ulpa particle separation model in a spiral classifier. State Higher Educational Institution National Mining University Ukraine: Natsional'nyi Hirnychyi Universytet Naukovyi Visnyk; 2020. pp. 31-35.
4. Lee S, Siegel JB, Stefanopoulou AG, Lee JW, Lee TK. Electrode state of health estimation for lithium ion batteries considering half-cell potential change due to aging. J Electrochem Soc. 2020; 167: 090531.
5. Reniers JM, Mulder G, Howey DA. Review and performance comparison of mechanical-chemical degradation models for lithium-ion batteries. J Electrochem Soc. 2019; 166: A3189.
6. Anseán D, García VM, González M, Blanco-Viejo C, Viera JC, Pulido YF, et al. Lithium-ion battery degradation indicators via incremental capacity analysis. IEEE Trans Ind Appl. 2019; 55: 2992-3002.
7. Prosser R, Offer G, Patel Y. Lithium-ion diagnostics: The first quantitative in-operando technique for diagnosing lithium ion battery degradation modes under load with realistic thermal boundary conditions. J Electrochem Soc. 2021; 168: 030532.
8. Beshta OS, Fedoreiko VS, Palchyk AO, Burega NV. Autonomous power supply of the objects based on biosolid oxide fuel systems. State Higher Educational Institution National Mining University Ukraine: Naukovyi Visnyk Natsionalnoho Hirnychoho Universytetu; 2015. pp. 67-73.
9. How DN, Hannan MA, Lipu MH, Ker PJ. State of charge estimation for lithium-ion batteries using model-based and data-driven methods: A review. IEEE Access. 2019; 7: 136116-136136.
10. Golovchenko A, Dychkovskyi R, Pazynich Y, Edgar CC, Howaniec N, Jura B, et al. Some aspects of the control for the radial distribution of burden material and gas flow in the blast furnace. Energies. 2020; 13: 923. doi: 10.3390/en13040923.
11. Beshta OO. Control of energy flows in electric drivetrain of electric vehicle with extra DC source. State Higher Educational Institution National Mining University Ukraine: Naukovyi Visnyk Natsionalnoho Hirnychoho Universytetu; 2019. pp. 67-71.
12. Beshta A, Aziukovskyi O, Balakhontsev A, Shestakov A. Combined power electronic converter for simultaneous operation of several renewable energy sources. Proceedings of the 2017 International Conference on Modern Electrical and Energy Systems (MEES); 2017 November 15th; Kremenchuk, Ukraine. Piscataway: IEEE.